LA-UR- 00-1900

Title: THE CONTOUR METHOD: SIMPLE 2-D MAPPING OF RESIDUAL STRESSES

Author(s): Michael B. Prime ESA-EA (prime@lanl.gov)
Antonio R. Gonzales ESA-WMM

Submitted to: Sixth International Conference on Residual Stresses
July 10-12, 2000
Oxford, UK
Proceedings, Volume 1, pp. 617-624.

THE CONTOUR METHOD: SIMPLE 2-D MAPPING OF RESIDUAL STRESSES

MB Prime and AR Gonzales
Engineering Sciences & Applications Division
Los Alamos National Laboratory
Los Alamos, NM 87545
prime@lanl.gov

ABSTRACT

We present an entirely new method for measuring residual stress that is extremely simple to apply yet more powerful than existing techniques. In this method, a part is carefully cut in two. The contour of the resulting new surface is measured to determine the displacements normal to the surface caused by the release of the residual stresses. Analytically, the opposite of these measured displacements are applied as boundary conditions to the surface in a finite element model. By Bueckner's superposition principle, this gives the original residual stresses normal to the plane of the cut. Unlike other relaxation methods for measuring residual stress, the measured data can be used to solve directly for the stresses without a tedious inversion technique. At the same time, an arbitrary two-dimensional variation in stresses can be determined. We demonstrate the method on a steel specimen with a known residual stress profile.

INTRODUCTION

The state-of-the-art residual stress measurement methods are significantly limited in their ability to measure spatial stress variations. In relaxation methods, the original stresses are determined from deformations measured after material removal. Only by removing material incrementally and making simplifying assumptions can one determine the spatial stress variation. Analytical complexity generally limits such techniques to measurement of one-dimensional (1-D) stress variations, e.g., incremental hole drilling (1) and crack compliance (2). Fundamentally, the analytical complexity occurs because the deformations are measured remote from the location of stress relief, e.g. on a pre-existing free surface.

The new relaxation technique presented in this work (3) can determine 2-D variations in residual stress without simplifying assumptions about the nature of the spatial variation. At the same time, the analysis to solve for the stresses from the measurements is exceedingly simple. These advances are possible because deformation is measured on the surface created by a cut, the location of stress relief, rather than on a pre-existing free surface.

The only common methods that can measure similar 2-D stress maps have significant limitations (4). The neutron diffraction method is nondestructive but sensitive to microstructural changes (5), time consuming, and limited in maximum specimen size, about 50 mm, and minimum spatial resolution, about 1 mm. Sectioning methods (e.g., 6) are experimentally cumbersome, analytically complex, error prone, and have limited spatial resolution, about 1 cm.

THEORY

The contour method for measuring residual stresses is based on a variation of Bueckner's superposition principle (7). Figure 1 presents an illustration in 2-D for simplicity, although the principle applies equally in 3-D. In **A**, one starts with our part containing the residual stresses to be determined. In **B**, the part has been cut in two, and the part has deformed because of the relieved residual stresses. In **C**, the free surface created by the cut is forced back to its original configuration from a stress-free starting point. Superimposing the stress states in **B** and **C** gives the original stress state. This superposition principle assumes that the material behavior is linearly elastic and that the material removal process does not introduce significant stresses.

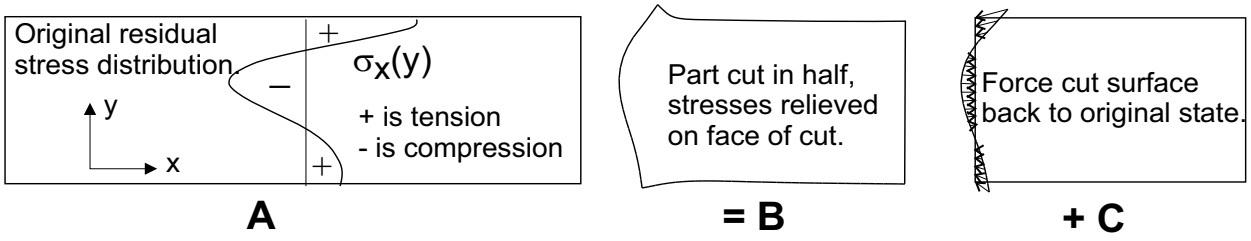

Figure 1. Superposition principle used to calculate original residual stress from measurement of surface contour after cutting a part in two.

Proper application of this superposition principle allows one to experimentally determine the residual stresses along the plane of the cut. Experimentally, the contour of the free surface is measured after the cut. Analytically, the surface of a stress-free model is forced back to its original configuration as in step **C**. Because the stresses in **B** are unknown, one cannot obtain the original stresses throughout the body. However, the stresses normal to the free surfaces in **B** must be zero. Therefore, step **C** by itself will give the correct stresses along the plane of the cut.

Experimentally, there is an arbitrary displacement in the contour measurement, i.e., the zero is arbitrary. There is also an arbitrary rotation in 2-D and two arbitrary rotations in 3-D. However, the arbitrary motions can be determined analytically by the need for the residual stresses to satisfy force and moment equilibrium. In fact, an FEM model used to solve for the stresses automatically accounts for the arbitrary motions, as will be demonstrated.

Measurement of the surface contour provides information about the displacements in the normal (x) direction only, not about those in the transverse (y) direction. Therefore, the analytical approximation of step **C** will force the surface back to its original configuration in the x-direction only, leaving the y-displacements unconstrained. If the residual shear stresses were zero along the plane of the cut, the approximation is exact: Poisson contractions will return the surface to its original y-position. In the general case, one assumes that the shear stresses on the cut plane are small. Similar assumptions are made by other proven measurement techniques, including hole drilling and sectioning methods (4). Qualitatively, this assumption is reasonable because the shear stress magnitude is limited by the free surface condition, the 2-D local equilibrium condition, $\partial\sigma_x/\partial x + \partial\tau_{xy}/\partial y = 0,$ and the need to satisfy net cross-section equilibrium. If σ_x is uniform in the x-direction, which is a reasonable assumption for many situations, the shear stresses must be zero. The errors caused by non-zero shear stresses will be assessed by numerical simulation in the next section of this paper.

A few researchers have applied a similar superposition principle before (8,9,10). However, they measured 1-D *approximations* of the contour on *pre-existing* free surfaces. A 3-D FEM simulation (11) showed that large errors resulted from such simplifications.

NUMERICAL VERIFICATION

An FEM simulation demonstrated the validity of the contour method and quantified the errors caused by the possible presence of shear stresses. A 2 × 1 beam was modeled using the ABAQUS commercial finite element code and a 40 × 20 mesh of 8-noded, quadratic shape function, plane stress elements (CPS8). The material behavior was isotropic linear elastic with an elastic modulus of 1000 and Poisson's ratio of 0.3. Residual stresses were initialized using a user subroutine, and one analysis step was performed to ensure initial equilibrium. A second analysis step removed the elements on the right half of the beam to simulate separating the part.

The first simulation considered the beam having no shear stresses along the plane of the cut. The axial residual on the plane of the cut, where the beam thickness goes from $y = 0$ to 1, were given by a simple parabolic distribution that satisfied equilibrium:

$$\sigma_x(y) = 6y^2 - 6y + 1 \quad . \tag{1}$$

Figure 2 shows that applying the contour method to the beam simulation gave the correct results. To apply the superposition principle, a model of the undeformed and unstressed half of the beam was taken from the full mesh. The displacements of the cut surface from the initial FEM model were applied with opposite sign as constraints to the nodes along the cut surface. Applying only the *x*-displacements, as would be the case with experimental implementation of the contour method, gave the correct stresses along the cut plane. Applying both *x*- and *y*-displacements gave identical results because the *y*-constraints gave zero constraint forces and the Poisson contraction automatically resulted in the correct transverse displacements.

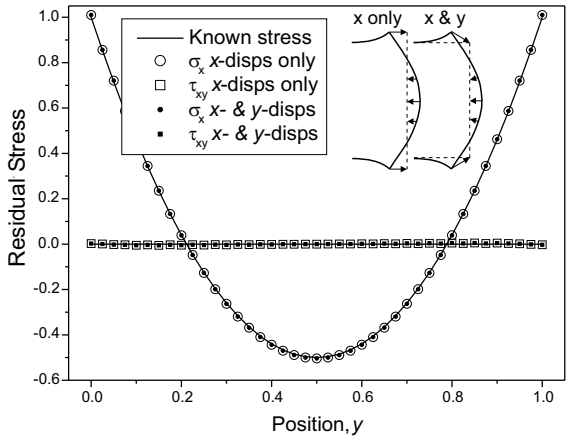

Figure 2. Simulation results, no shear stress.

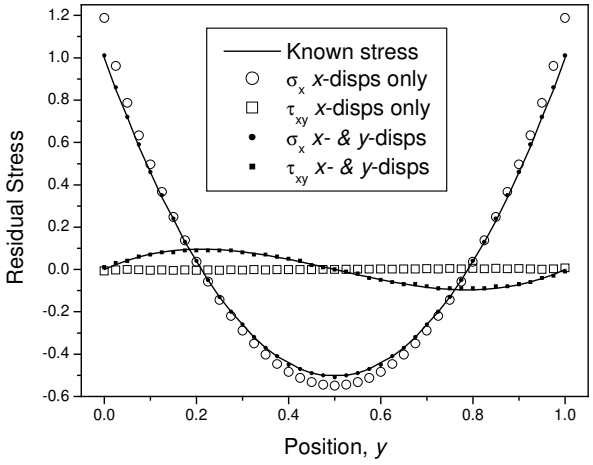

Figure 3. Simulation results, with shear stress.

The second simulation considered a beam with shear stresses along the plane of the cut. The

axial stresses along the plane of the cut were still given by Eq. (1) but were varied in the *x*-direction to give $\partial\sigma_x(x, y)/\partial x = -\sigma_x$. Combined with the equilibrium condition and free surface conditions, this $\partial\sigma_x(x, y)/\partial x$ results in a shear stress distribution on the cut plane of

$$\tau_{xy}(y) = \left(2y^3 - 3y^2 + y\right). \qquad (2)$$

Figure 3 shows the small errors that resulted from applying the contour method when shear stresses were present on the cut plane. Applying both the *x*- and *y*-displacements to the surface gave the correct results for both normal and shear stresses. However, experimentally we would only be able to determine the normal (*x*) displacements. Applying just the *x*-displacements gave a root-mean-square error in the σ_x distribution of 0.059, or 5.9% of the peak value. As expected, application of only *x*-displacements gave zero shear stresses.

The shear stress simulation is a pessimistic case, and yet the errors were quite small. Because of the free surface conditions and equilibrium condition, the magnitude of $\partial\sigma_x(x, y)/\partial x$ determines the maximum value of shear stress. For our simulated beam, σ_x decays from its peak value to zero in about one beam thickness. By St. Venant's principle, one expects such changes near the ends of a body. However, the stresses can reasonably be expected to be much more constant in the central region of many bodies, resulting in lower shear stresses.

EXPERIMENTAL VALIDATION

Known Residual Stress Specimen. A plastically bent beam was carefully prepared in order to provide a specimen with a known residual stress profile. 43 mm square stock of forged 21Cr-6Ni-9Mn austenitic stainless steel was annealed at 1080°C for one hour and argon quenched. Next, the beam was machined to final shape with a 30 mm × 10 mm minimum cross section. Then the beam was thoroughly stress relieved by heating in a vacuum to 1080°C for 15 minutes and slow cooling at 100°C per hour. The beam was then plastically bent and unloaded in a carefully designed four-point bend fixture (12) to a maximum outer fiber strain of about 5670 με. Strain and load measurements during bending were used to calculate independent stress-strain curves for loading and unloading in both tension and compression (12). Finally, superposition of these curves gave the residual stress profile. The elastic modulus determined during these tests was 194 GPa.

Experiment. For the contour method, the ideal machining process for separating the part would make a precisely straight cut and not introduce any plastic deformation. Wire electric discharge machining (wire EDM) is probably the choice closest to the ideal (13). In wire EDM, a wire is electrically charged with respect to the workpiece, and spark erosion causes material removal. The cutting is noncontact, whereas conventional machining causes localized plastic deformation from the large contact forces. The wire-control mechanisms can achieve positional precision of a fraction of a micrometer, especially for a straight cut. For this test, the beam was cut with a Mitsubishi SX-10 machine and a 100 μm diameter zinc-coated wire. "Skim cut" settings, which are normally used for better precision and a finer surface finish, were used because they also minimize any recast layer and cutting-induced stresses (13,14). Including the kerf, the slot was about 140 μm wide.

The beam had to be fixed firmly enough to prevent unwanted movement during cutting, which required that the beam be clamped on both sides of the cut. Usually with wire EDM only one side is clamped. To assure that no thermal stresses would arise, the beam and all the clamps were allowed to come to thermal equilibrium in the water before they were secured.

The contour of the cut surface was measured using a Brown & Sharpe XCEL 765 coordinate measuring machine (CMM), which resides in a temperature and humidity controlled inspection laboratory. A CMM uses a touch trigger probe to register mechanical contact. An optoelectric system using glass scales gives the probe location, which is combined with machine coordinates to locate the surface. Because the CMM uses a probe tip with a finite radius, surface roughness and porosity are at least partially filtered out from the measured contour. A 4 mm diameter ruby tip was selected after trial measurements using tips with diameters from 1 mm to 8 mm revealed no significant measurement differences.

Figure 4 shows 1-D contours measured on the cut surfaces from both halves of the beam. The zeros are arbitrary, so the offset between the two curves is irrelevant. The measurements were taken in the center of the surface, and $y = 0$ represents the beginning of the cut. Additional traces taken off from the center showed very similar data. For both surfaces, positive x is taken in the outward normal direction; therefore, values that are more positive represent higher regions of the surface. 2-D measurements were also taken over the entire surface using the CMM and a 50 by 300 grid.

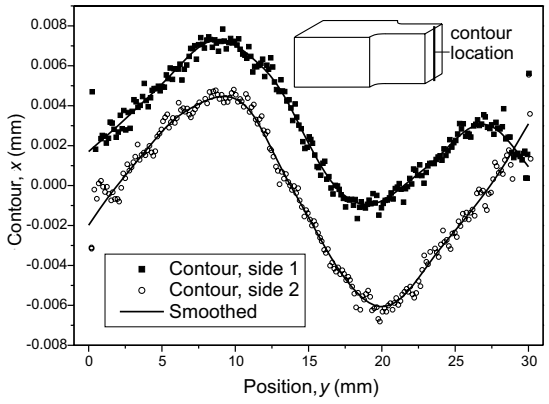

Figure 4. Surface contour measured on both halves of the beam.

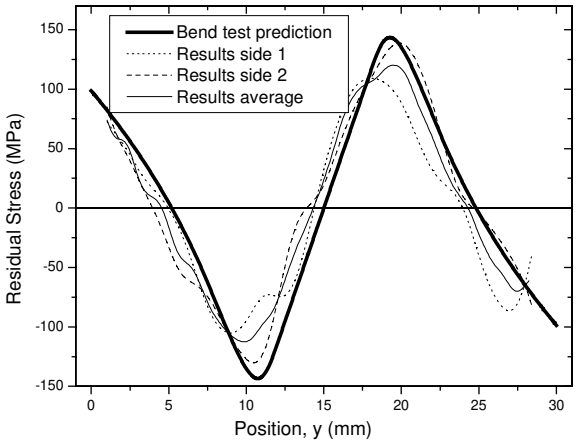

Figure 5. Results from applying 1-D contour to 2-D finite element model.

Calculations. For simplicity, the initial calculations were performed on only a 2-D model using the measurements shown in Fig. 4. The half-beam was modeled using a 30×78 mesh of 8-noded, quadratic shape function, plane stress elements (CPS8). The material behavior was isotropic linearly elastic with an elastic modulus of 194 GPa and Poisson's ratio of 0.28. After careful smoothing of the data, the opposite of the measured contour was applied as displacement boundary conditions to the nodes on the surface representing the cut.

Figure 5 shows the 1-D residual stress profiles measured by the contour method compared with the prediction from the bend test. The results were obtained by post-processing the FEM results to extrapolate σ_x to the nodes along the surface representing the cut. Because the measured displacement contours from Fig. 4 had to be extrapolated slightly to cover the full range, the results are truncated near the ends. The agreement with the prediction is striking, especially considering the low magnitude of residual stresses. Such low residual stresses in a stiff material like steel result in a lower magnitude of the contour and, therefore, increased errors.

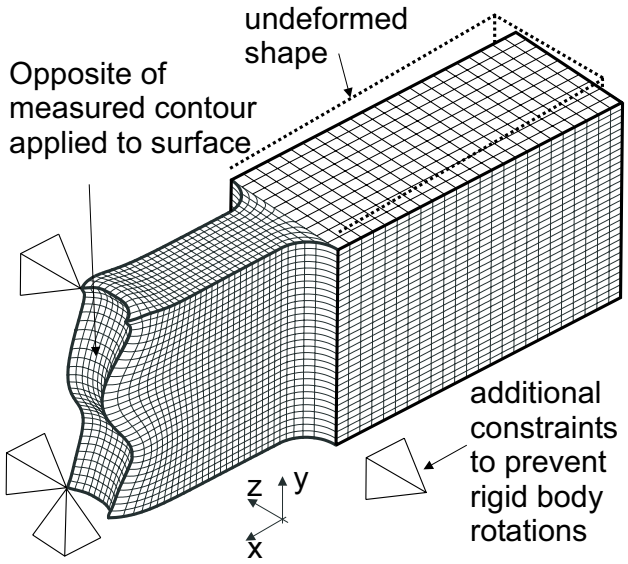

Figure 6. Applying 2-D measured surface contour to 3-D beam model.

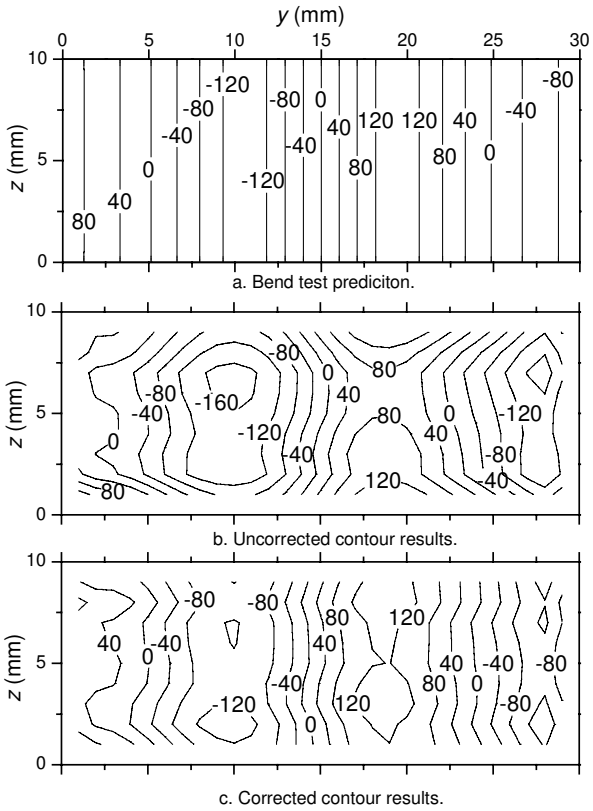

Figure 7. Measured stress map compared to prediction.

To illustrate the ability of the contour method to measure a full 2-D stress map, the contour measured on the entire cut surface was applied to a 3-D model. The half-beam was modeled in ABAQUS using 16,200 20-noded, quadratic shape function brick elements (C3D20). This mesh gave a 10 × 30 mesh of elements on the 10 mm × 30 mm cut surface. The measured surface contour data was fit to a bivariate Fourier series, averaged between sides one and two, and then applied as displacement boundary conditions in the FEM model. Figure 6 shows the deformed finite element model and the three displacement constraints used to prevent rigid body motions. As discussed previously, the FEM solution easily handled the arbitrary displacement and rotation in the measured contour. The movement of the free end of the beam illustrates the rotation necessary to satisfy moment equilibrium and the slight contraction to satisfy force equilibrium.

Figure 7 shows the measured 2-D map of residual stresses compared to the bend test prediction. Because the surface contour measured on the CMM had to be extrapolated slightly to the edges of the surface, the contour lines are not plotted all the way to the edges. The agreement between measurement, Fig. 7b, and prediction, Fig. 7a, is good. However, the z-direction curvature in the measured contour, see Fig. 6, resulted in a small shift in the calculated stresses towards more compressive values along the center of the surface (z = 5). As will be discussed, that curvature results from using sub-optimal settings during the wire EDM cutting. Therefore, it was corrected for in a simple manner by fitting the curvature at y = 15 and then subtracting this curvature from the entire surface. Figure 7c shows the corrected results. The agreement with prediction is now very good, similar to the results in Fig. 5.

DISCUSSION

First we briefly mention that analytical smoothing of the measured contour is crucial because calculating stress from the displacements amplifies any noise in the data.

The contour method is sufficiently sensitive to measure residual stress maps of interest. The beam specimen in this study could be considered a sensitivity test because the stresses were less than 150 MPa and resulted in a contour with only about a 10 μm peak-to-peak magnitude. Residual stresses are often several times greater, the parts are also often larger, and many materials of interest have lowed elastic moduli, any of which would give larger contours. Some preliminary measurements on a 38-mm thick butt-welded steel plate gave a contour of about 120 μm peak-to-peak magnitude. Future work will, however, need to consider the effect of plasticity on the contour method for stresses near the yield strength.

Errors can be greatly reduced by correctly clamping the specimen during the cutting. The cut is assumed to occur along a flat plane in the original configuration. However, stress relief causes this plane to move slightly as the cut progresses. Such movement can be quantified using a simple FEM model. When the specimen is clamped on both sides of the cut, the resulting error in the stress distribution is less than 10%. More sophisticated clamping arrangements could probably reduce the errors further. Initial simulations suggest that errors can be minimized in general by measuring the contour on both halves of any specimen and using the average in calculations.

The z-direction curvature in the measured surface contour, see Fig. 6, appears to be caused by a common source of inaccuracy in wire EDM machining called “barreling” (13). The barreling can be minimized by optimizing cutting parameters, such as by cutting more slowly. In addition, the barreling will have a reduced influence on measurement of larger residual stresses because it will make up a lesser portion of the measured contour.

CONCLUSIONS

The contour method of measuring residual stress was experimentally validated using a bent beam specimen. In many ways, the contour method surpasses other measurement methods in both ability to measure stresses and ease of use:

1. The contour method can measure a full 2-D map of the residual stress component normal to the cross section.

2. The residual stress map can be obtained directly from the measured contour; no inverse procedure or assumptions about the stress variations are necessary.
3. The technique is experimentally simple. No strain gages or other instrumentation is required during the testing. The necessary equipment is widely available in machine shops and inspection laboratories.

The contour method has the potential to measure residual stress maps that are extremely difficult to measure with other techniques. One particularly promising application is welding residual stresses. Microstructural changes in the weld material make neutron diffraction measurements difficult (5) but have relatively small effects on the elastic constants that would affect the contour method. Other exciting applications include parts with geometrically complex cross sections, like railroad rails, forgings, I-beams, extrusions, and castings.

ACKNOWLEDGEMENTS

This work was performed at Los Alamos National Laboratory, operated by the University of California for the U. S. Department of Energy under contact number W-7405-ENG-36.

REFERENCES

1. Schajer GS, Journal of Engineering Materials and Technology 110 (1988) 338–349.
2. Cheng W, Finnie I, Journal of Engineering Materials and Technology 108 (1986) 87–92.
3. Prime MB, "2-D Mapping of Residual Stresses by Measuring the Surface Contour After a. Cut," Journal of Engineering Materials and Technology (submitted).
4. Lu J, James M, Roy G, 'Handbook of Measurement of Residual Stresses', The Fairmont Press, Inc. (Lilburn, Georgia, USA) 1996.
5. Krawitz AD, Winholtz RA, Materials Science and Engineering A-Structural Materials Properties Microstructure and Processing 185, (1994) 123–130.
6. Rybicki EF, Shadley JR, Journal of Engineering Materials and Technology 108 (1986) 99–106.
7. Bueckner HF, Transactions of the American Society of Mechanical Engineers 80 (1958) 1225–1230.
8. Williams JF, Stouffer DC, Engineering Fracture Mechanics 11 (1979) 547–557.
9. Johnson MR, Robinson RR, Opinsky AJ, Joerms MW, Stone DH., paper 85-WA/RT-17, The American Society of Mechanical Engineers (1985).
10. Dickson TL, Bass BR, McAfee WJ, PVP-373, Fatigue, Fracture, and Residual Stresses (1998) 387–395.
11. Lin KY, Huang JS, Theoretical and Applied Fracture Mechanics (12) (1989) 73–86.
12. Mayville RA, Finnie I, Experimental Mechanics 22 (1982) 197–201.
13. Sommer C, Sommer S, 'Wire EDM Handbook', Advance Publishing, Inc., (Houston, Texas, USA) 1997.
14. Cheng W, Finnie I, Gremaud M, Prime MB, Journal of Engineering Materials and Technology 116 (1994) 1–7.